Prompt photon and associated heavy quark production in the k_T-factorization approach

M.A. Malyshev

in collaboration with
A.V. Lipatov
N.P. Zotov

M.V. Lomonosov Moscow State University
D.V. Skobeltsyn Institute of Nuclear Physics

JHEP **1205** (2012) 104

Outline

1. Motivation
2. k_T-factorization approach
   - unintegrated parton distributions
   - off-shell matrix elements
3. Parameters
4. Numerical results
5. Conclusion

Motivation

Prompt photon and associated heavy (*b, c*) quark production is highly sensitive to parton distribution in the hadron. So it provides a test of hard subprocess dynamics.

In this work the k_T-factorization approach is used to make the calculations for the process. The essential ingredient of this method is unintegrated (transverse momentum dependent) parton distribution functions. One of the aims of the presented study was to test these parton densities. This is important as a step in the search of universal uPDFs.

Here we describe the experimental data for prompt photon and associated heavy quark production obtained by the D0 and CDF collaborations at the Tevatron. Also we make predictions for the LHC.

k_T-factorization approach

1. Unintegrated parton distributions
2. Matrix elements which depend on the transverse momenta of incoming partons.

Off-shell matrix elements

1. $g^*g^* \to \gamma Q\overline{Q}$
2. $q^*\overline{q}^* \to \gamma Q\overline{Q}$
3. $q^*Q \to \gamma qQ$

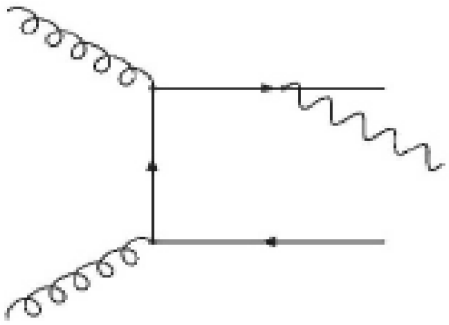

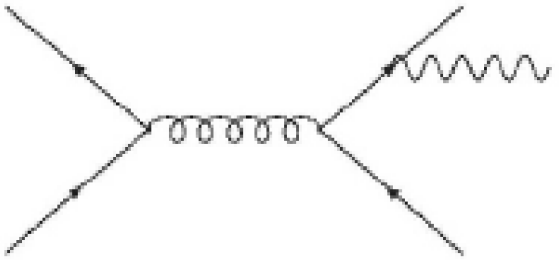

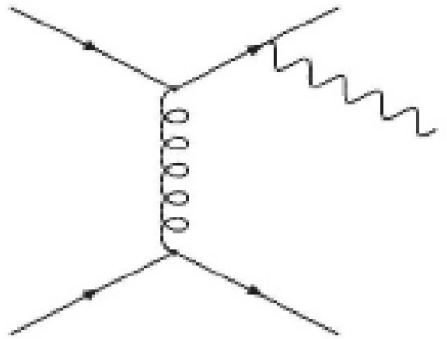

Unintegrated parton distributions

KMR approach(Kimber, Martin, Ryskin) [M.A. Kimber, A.D. Martin, M.G. Ryskin, Phys. Rev. D **63**, 114027 (2001); G. Watt, A.D. Martin, M.G. Ryskin, Eur. Phys. J. C 31, 73 (2003)]. Weakening of the strong ordering:

$$k_{1,T} \ll ... \ll k_{n-1,T} \ll k_T \sim \mu$$

Unintegrated parton distributions

In the KMR approach the distribution functions start to depend on the transverse momenta of the partons, and $f_a(x,\mathbf{k}_T^2)=const$, if $\mathbf{k}_T^2<\mu_0^2\sim1$ GeV^2, otherwise they take the form:

$$f_q(x,\mathbf{k}_T^2,\mu^2)=T_q(\mathbf{k}_T^2,\mu^2)\frac{\alpha_s(\mathbf{k}_T^2)}{2\pi}\times$$

$$\times\int_x^1 dz\left[P_{qq}(z)\frac{x}{z}q\left(\frac{x}{z},\mathbf{k}_T^2\right)\Theta\left(\Delta-z\right)+P_{qg}(z)\frac{x}{z}g\left(\frac{x}{z},\mathbf{k}_T^2\right)\right],$$

$$f_g(x,\mathbf{k}_T^2,\mu^2)=T_g(\mathbf{k}_T^2,\mu^2)\frac{\alpha_s(\mathbf{k}_T^2)}{2\pi}\times$$

$$\times\int_x^1 dz\left[\sum_q P_{gq}(z)\frac{x}{z}q\left(\frac{x}{z},\mathbf{k}_T^2\right)+P_{gg}(z)\frac{x}{z}g\left(\frac{x}{z},\mathbf{k}_T^2\right)\Theta\left(\Delta-z\right)\right],$$

As the input we use MSTW2008 set.

Parameters

- Significant theoretical uncertainties are connected with the choice of the factorization and renormalization scales. We took $\mu_R = \mu_F = \mu = \xi|\mathbf{p}_T|$ (ξ= 1, ½, 2).
- We neglected the light quarks masses.
- For completeness, we use LO formula for the strong coupling constant $\alpha_s(\mu^2)$ with n_f = 4 active quark flavours at Λ_{QCD} = 200 MeV, so $\alpha_s(M_z^2)$=0.1232.

Parameters

In order to reduce the huge background from the secondary photons produced by the decays of π_0 and η mesons the isolation criterion is introduced in the experimental analyses. This criterion is the following. A photon is isolated if the amount of hadronic transverse energy E_T^{had} deposited inside a cone with aperture R centered around the photon direction in the pseudo-rapidity and azimuthal angle plane, is smaller than some value E^{max}.

$$E_T^{had} \leq E^{max}$$

$$(\eta^{had} - \eta)^2 + (\varphi^{had} - \varphi)^2 \leq R^2.$$

The isolation cut not only reduces the background but also significantly reduces the so called fragmentation components, connected with collinear photon radiation (10%). We took $R=0.4$ and $E^{max} = 1$ GeV.

Numerical results

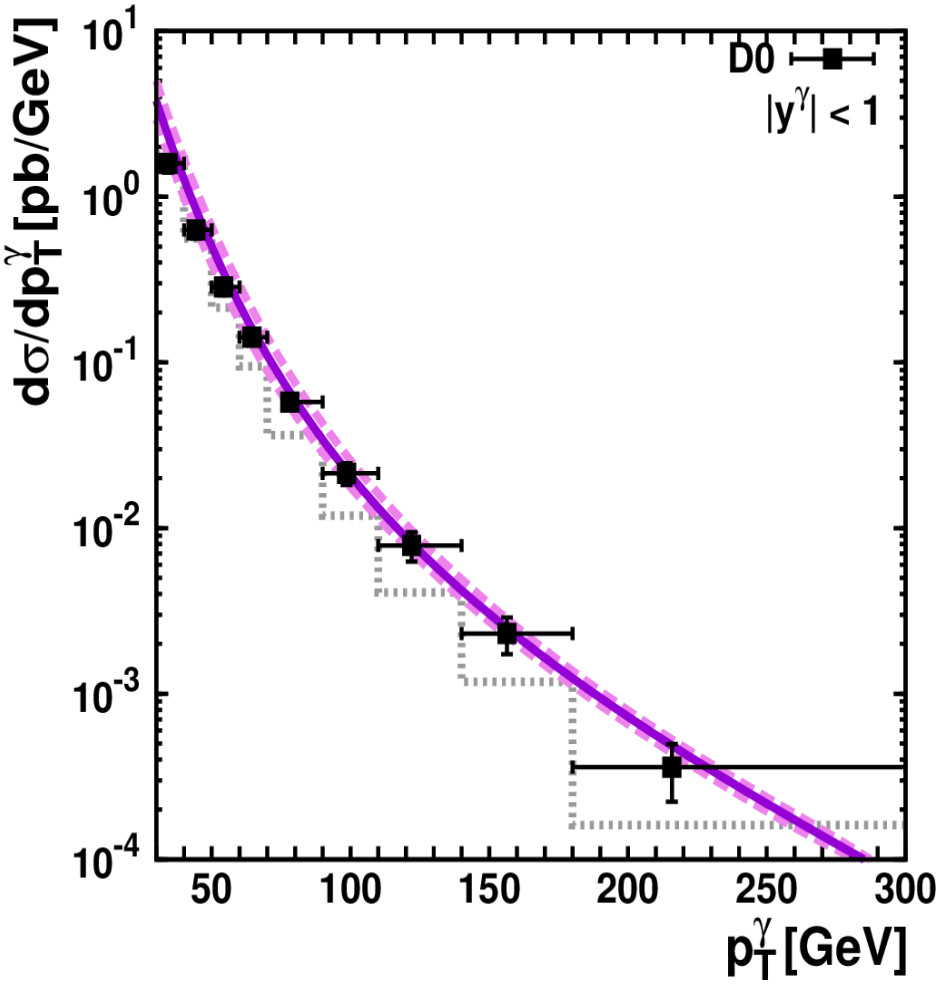

1. Differential cross section of associated prompt photon and b-jet production $p\bar{p} \to \gamma bX$ *at* Tevatron energies ($\sqrt{s}$=1.96 TeV). The experimental data are of D0 ($|y^{\gamma}|<1$, $|y^{b\text{-}jet}|<1.5$, $p_T^{b\text{-}jet}>15$ GeV). The dotted line represents the NLO pQCD predictions [Stavreva, Owens, 2009]

Numerical results

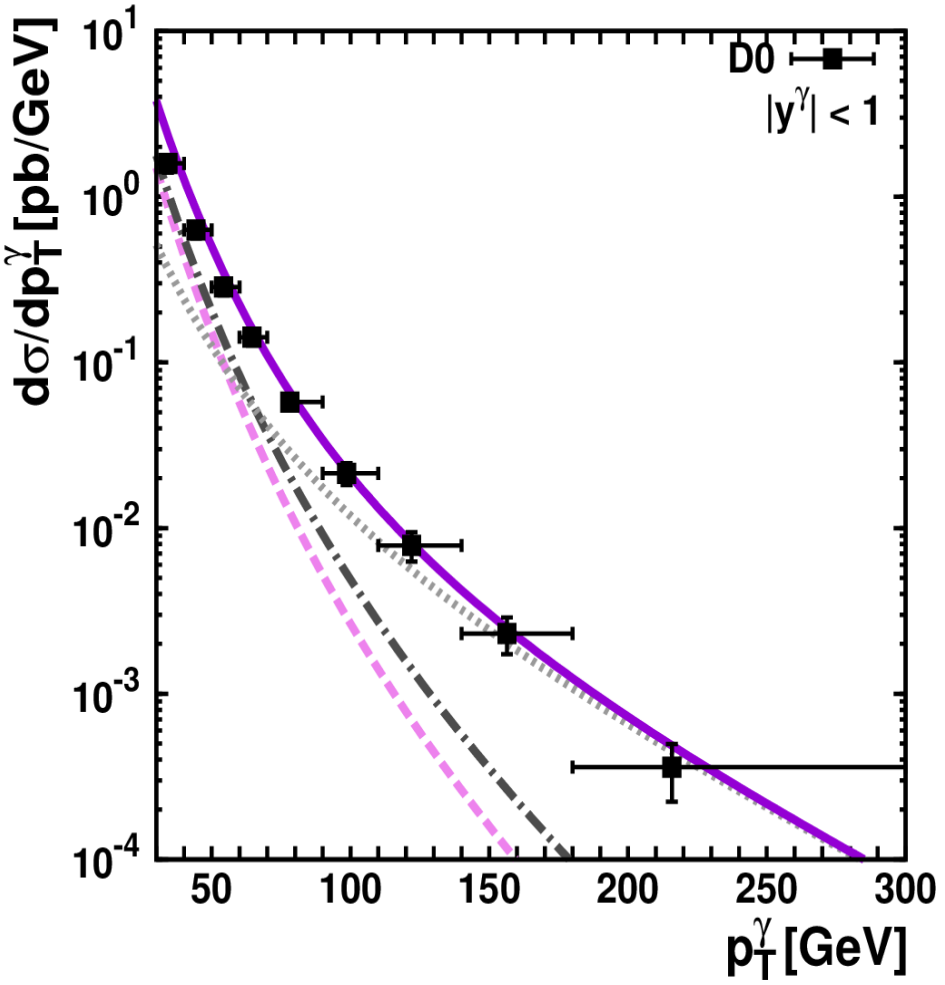

1. Differential cross section of associated prompt photon and b-jet production $p\bar{p} \to \gamma b X$ *at* Tevatron energies ($\sqrt{s}$=1.96 TeV). The experimental data are of D0 ($|y^{\gamma}|<1.5$, $|y^{b\text{-}jet}|<1.5$, $p_T^{b\text{-}jet}>15$ GeV). The dashed, dotted and dashed-dotted lines correspond to $g^*g^* \to \gamma b\bar{b}$, $q^*\bar{q}^* \to \gamma b\bar{b}$ *and* $q^*b \to \gamma qb$.

Numerical results

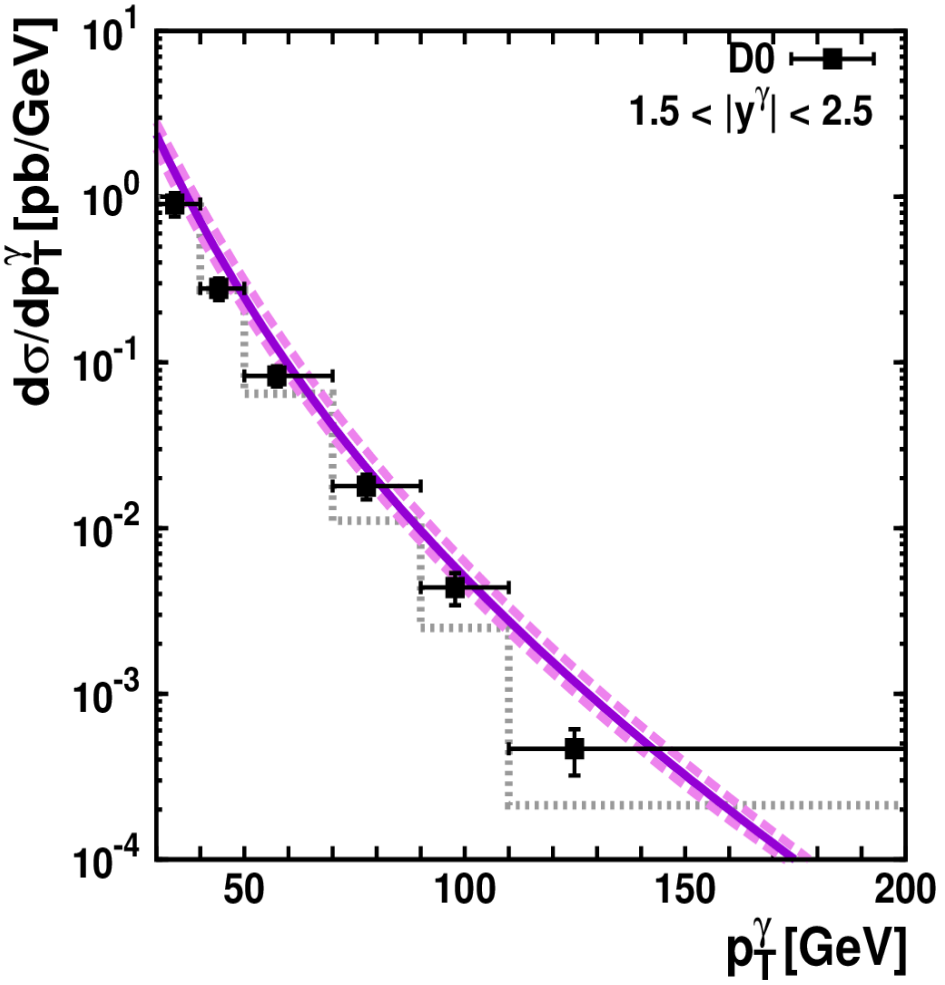

1. Differential cross section of associated prompt photon and b-jet production $p\bar{p}\rightarrow\gamma bX$ *at* Tevatron energies ($\sqrt{s}$=1.96 TeV). The experimental data are of D0 (*1.5*<|y^{γ}|<*2.5,* |$y^{b\text{-}jet}$|<*1.5,* $p_T^{b\text{-}jet}$>*15* GeV*)*. The dotted line represents the NLO pQCD predictions [Stavreva, Owens, 2009]

Numerical results

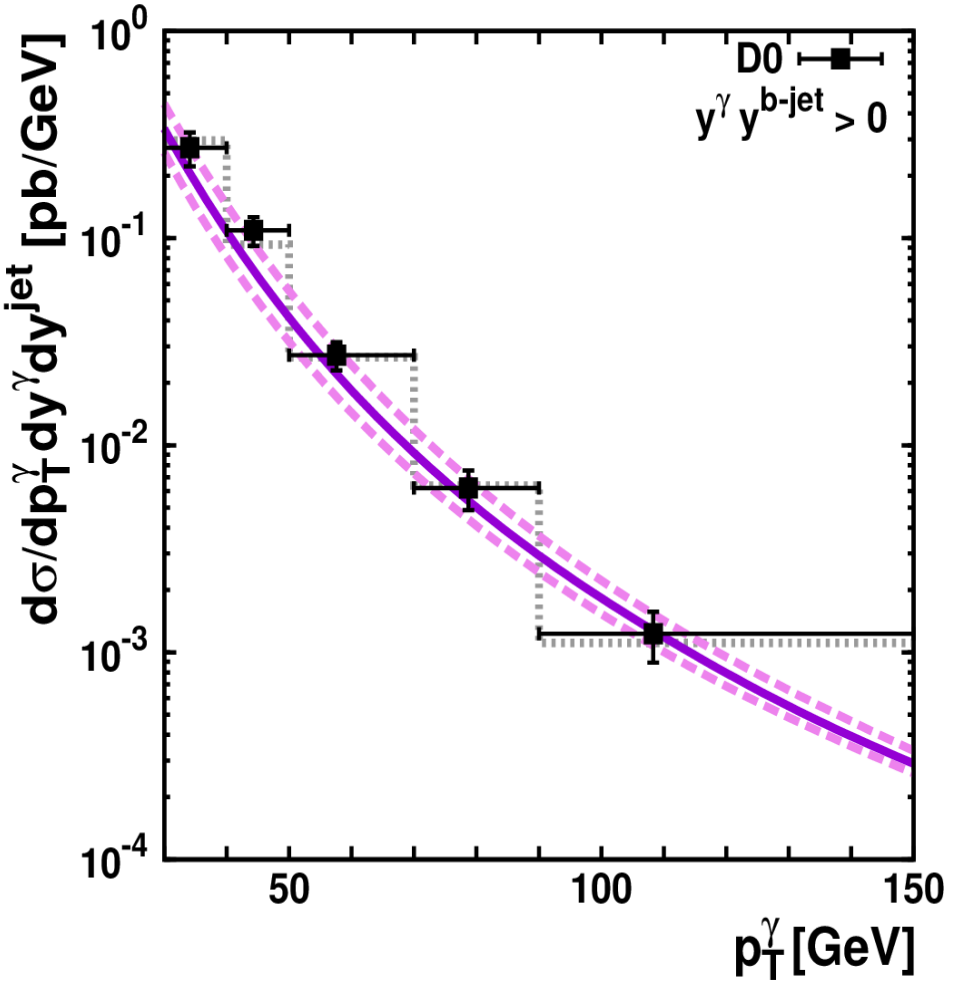

2. Differential cross section of associated prompt photon and b-jet production $p\bar{p}\rightarrow\gamma bX$ *at* Tevatron energies ($\sqrt{s}$=1.96 TeV). The experimental data are of D0 ($|y^\gamma y^{b\text{-jet}}|>0$, $|y^\gamma|<1$, $|y^{b\text{-jet}}|<0.8$, $p_T^{b\text{-jet}}>15$ GeV). The dotted line represents the NLO pQCD predictions [Stavreva, Owens, 2009]

Numerical results

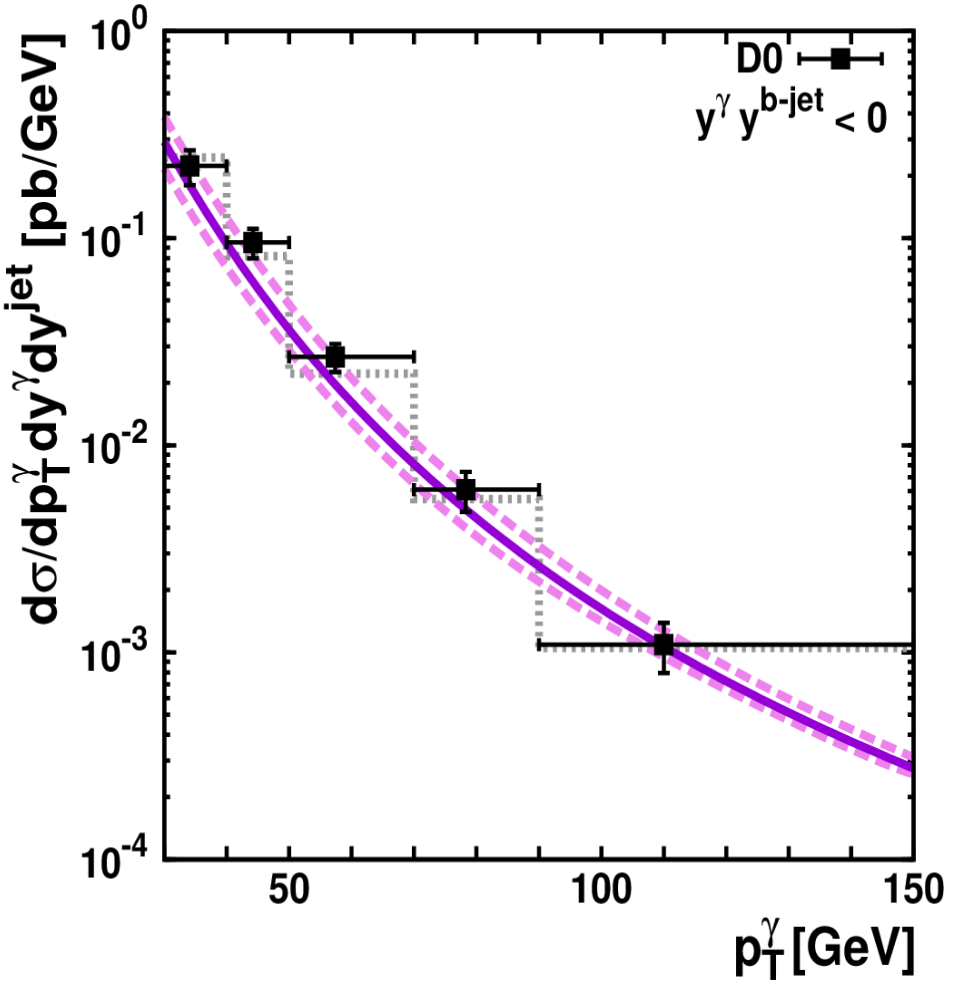

2. Differential cross section of associated prompt photon and b-jet production $p\bar{p}\rightarrow\gamma bX$ *at* Tevatron energies ($\sqrt{s}$=1.96 TeV). The experimental data are of D0 ($|y^\gamma y^{b\text{-jet}}|<0$, $|y^\gamma|<1$, $|y^{b\text{-jet}}|<0.8$, $p_T^{b\text{-jet}}>15$ GeV). The dotted line represents the NLO pQCD predictions [Stavreva, Owens, 2009]

Numerical results

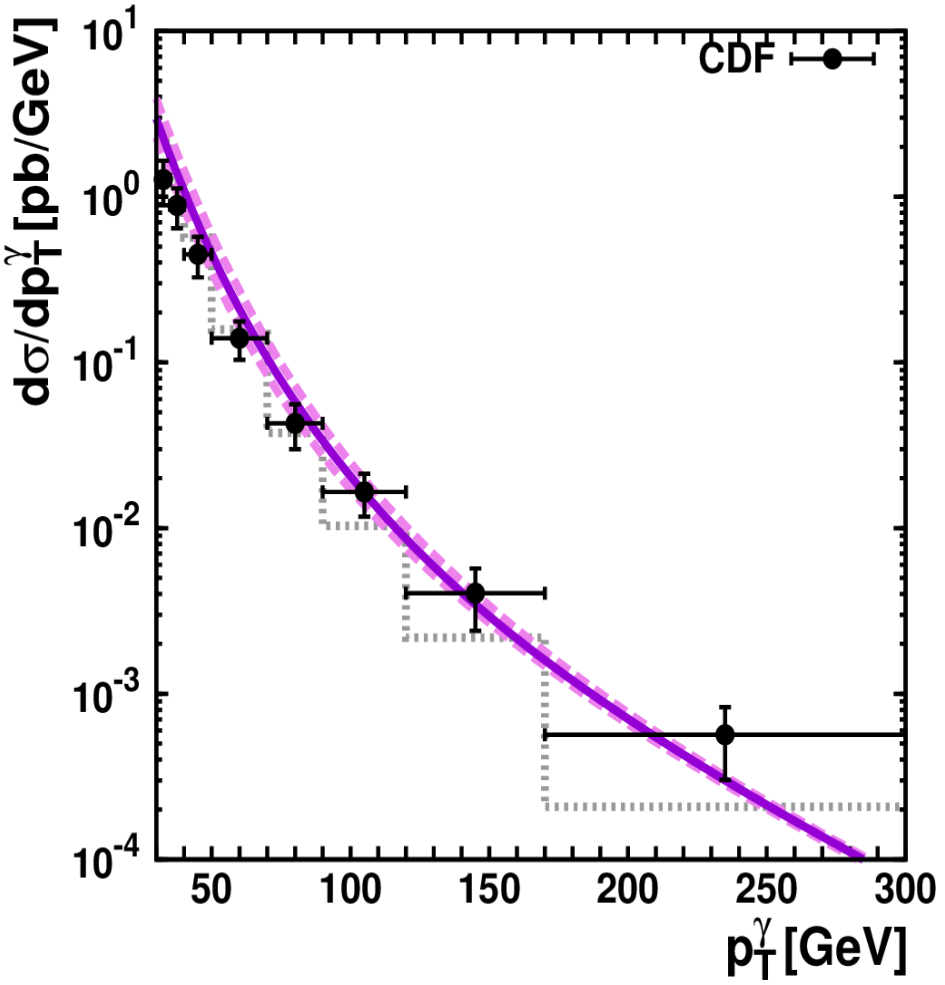

3. Differential cross section of associated prompt photon and b-jet production $p\bar{p} \to \gamma bX$ *at* Tevatron energies ($\sqrt{s}$=1.96 TeV). The experimental data are of CDF ($|y^\gamma|<1$, $|y^{b\text{-}jet}|<1.5$, $p_T^{b\text{-}jet}>20$ GeV). The dotted line represents the NLO pQCD predictions [Stavreva, Owens, 2009]

Numerical results

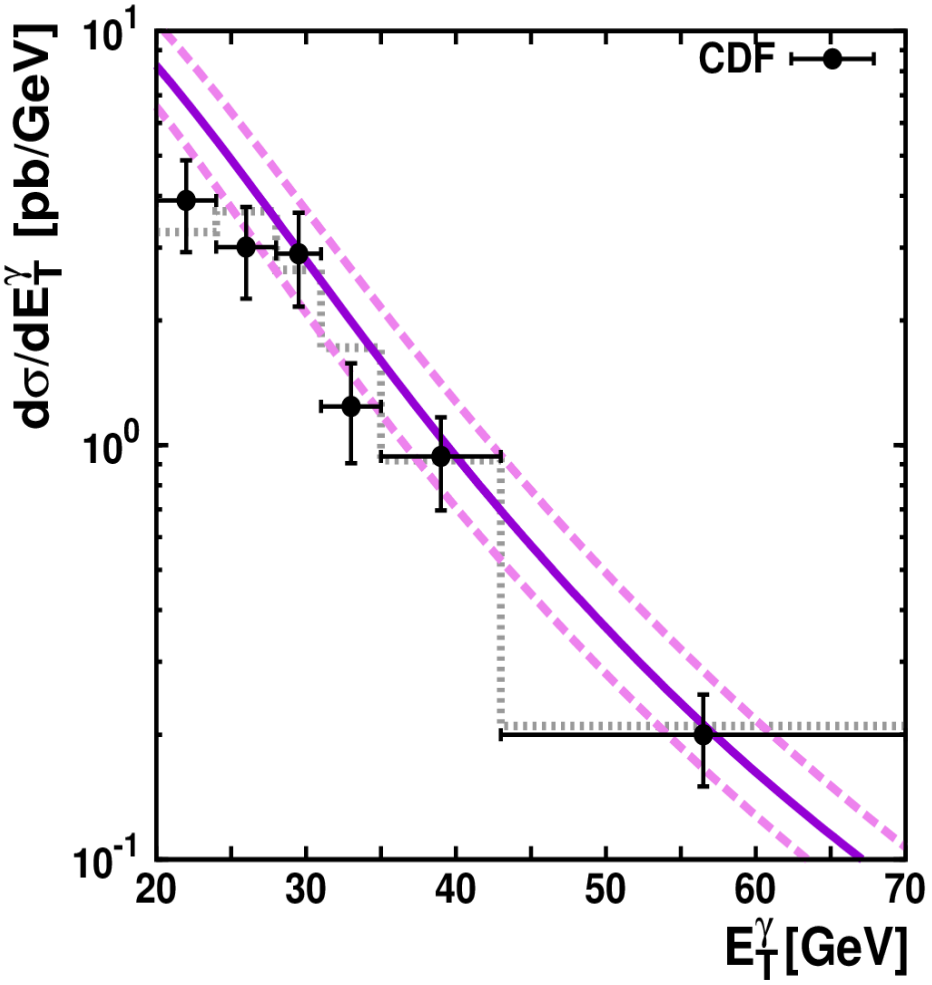

3. Differential cross section of associated prompt photon and b-jet production $p\bar{p} \to \gamma b X$ *at* Tevatron energies ($\sqrt{s}$=1.96 TeV). The experimental data are of CDF ($|\eta^\gamma|<1.1$, $|\eta^{b\text{-}jet}|<1.5$, $p_T^{b\text{-}jet}>20$ GeV). The dotted line represents the NLO pQCD predictions [Stavreva, Owens, 2009]

Numerical results

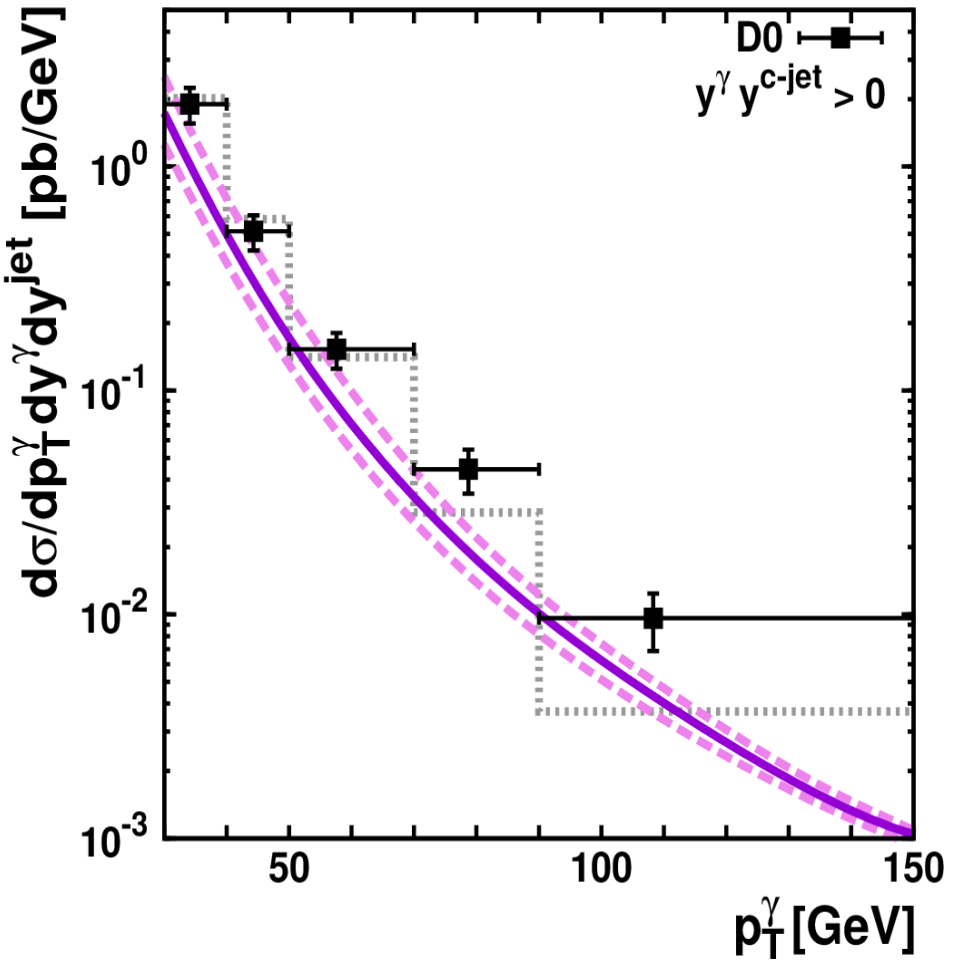

4. Differential cross section of associated prompt photon and c-jet production $pp \to \gamma cX$ *at* Tevatron energies ($\sqrt{s}$=1.96 TeV). The experimental data are of D0 ($|y^{\gamma}y^{c\text{-jet}}|>0$, $|y^{\gamma}|<1$, $|y^{c\text{-jet}}|<0.8$, $p_T^{c\text{-jet}}>15$ GeV). The dotted line represents the NLO pQCD predictions [Stavreva, Owens, 2009]

Numerical results

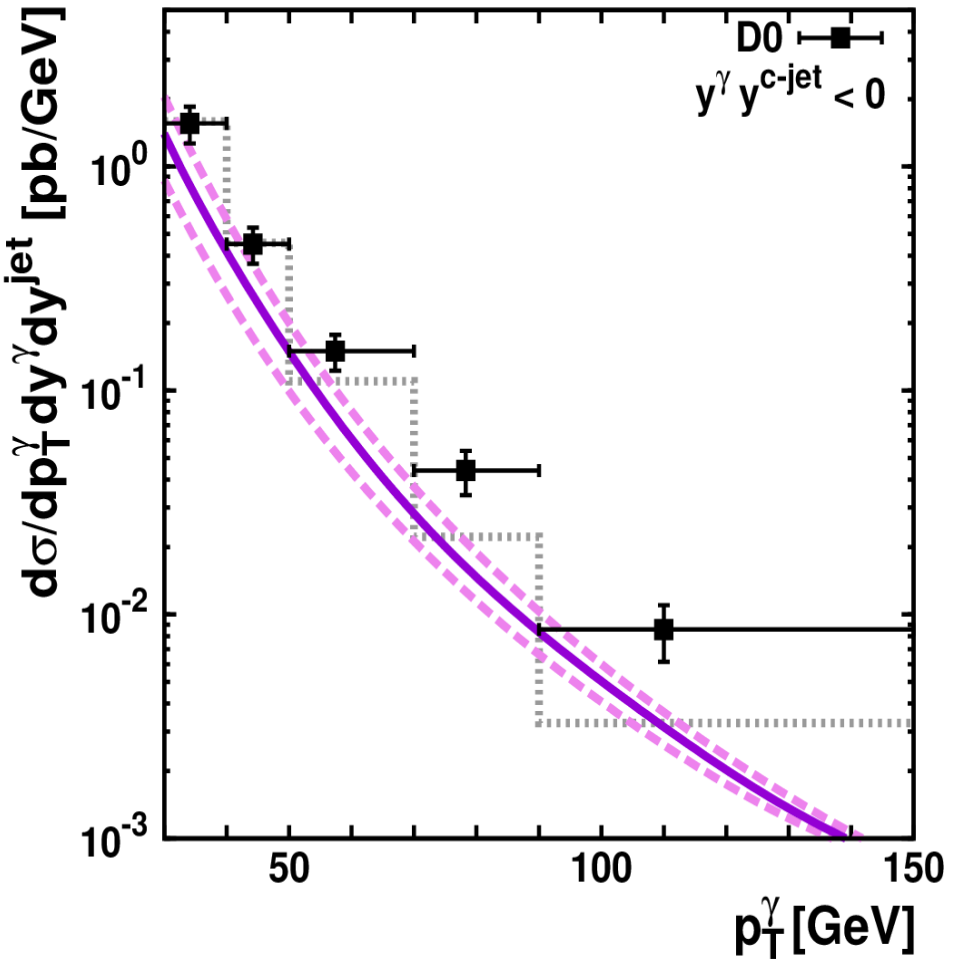

4. Differential cross section of associated prompt photon and c-jet production $p\bar{p} \to \gamma cX$ *at* Tevatron energies ($\sqrt{s}$=1.96 TeV). The experimental data are of D0 ($|y^\gamma y^{c\text{-jet}}|<0$, $|y^\gamma|<1$, $|y^{c\text{-jet}}|<0.8$, $p_T^{c\text{-jet}}>15$ GeV). The dotted line represents the NLO pQCD predictions [Stavreva, Owens, 2009]

Numerical results

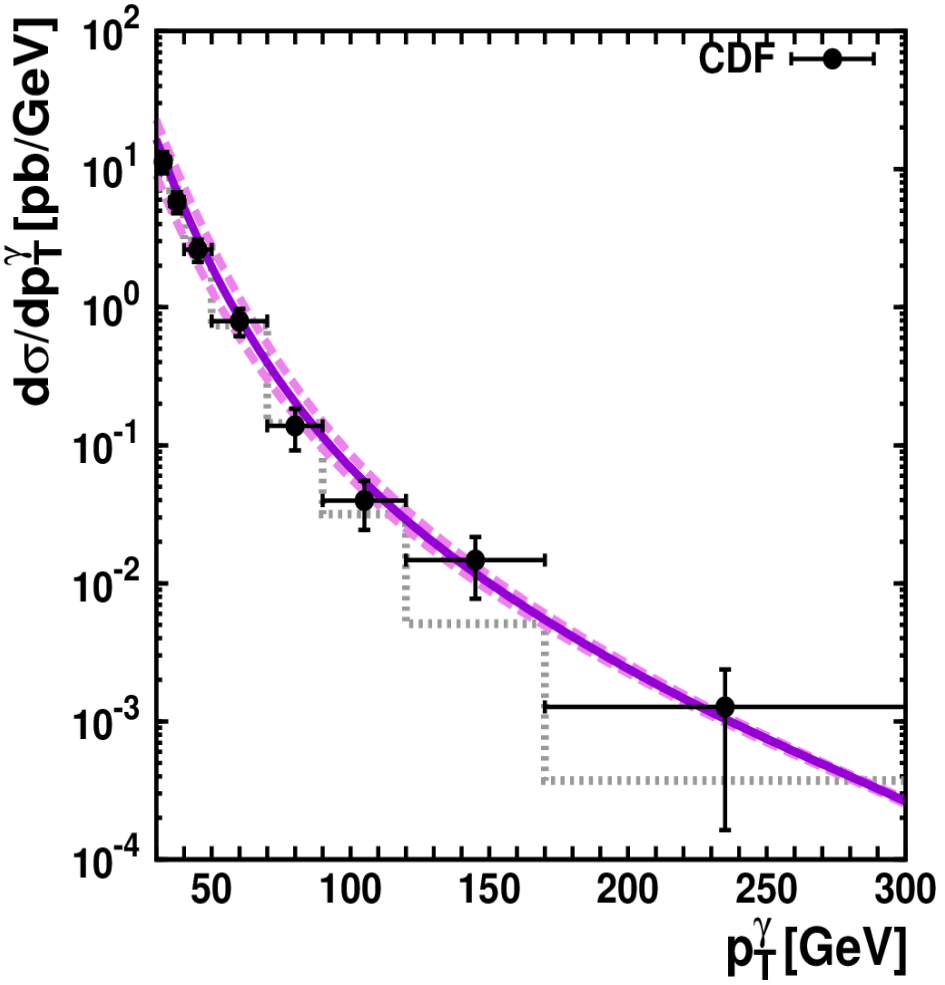

5. Differential cross section of associated prompt photon and c-jet production $p\bar{p} \to \gamma cX$ *at* Tevatron energies ($\sqrt{s}$=1.96 TeV). The experimental data are of CDF ($|y^\gamma|<1$, $|y^{c\text{-}jet}|<1.5$, $p_T^{c\text{-}jet}>20$ GeV). The dotted line represents the NLO pQCD predictions [Stavreva, Owens, 2009]

Numerical results

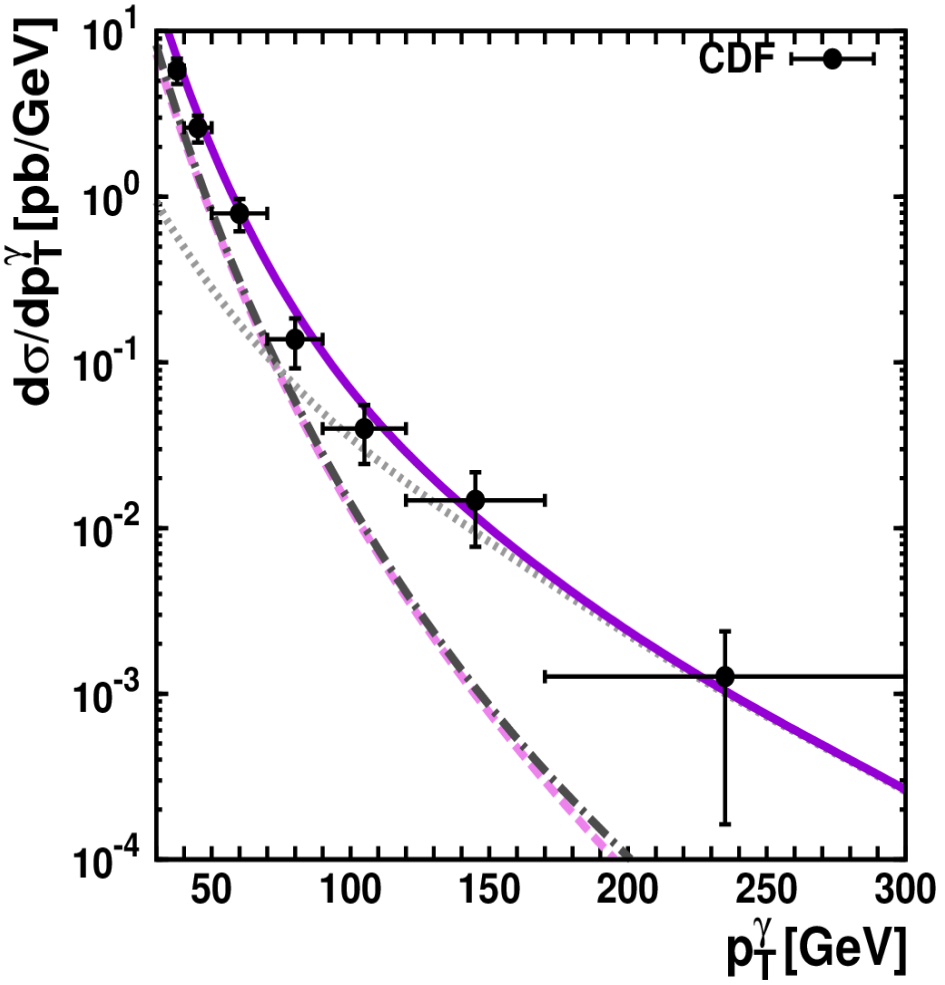

5. Differential cross section of associated prompt photon and c-jet production $pp \to \gamma cX$ at Tevatron energies ($\sqrt{s}$=1.96 TeV). The experimental data are of CDF ($|y^\gamma|<1$, $|y^{c\text{-}jet}|<1.5$, $p_T^{c\text{-}jet}>20$ GeV). The dashed, dotted and dashed-dotted lines correspond to $g^*g^* \to \gamma c\bar{c}$, $q^*\bar{q}^* \to \gamma c\bar{c}$ and $q^*c \to \gamma qc$.

Numerical results

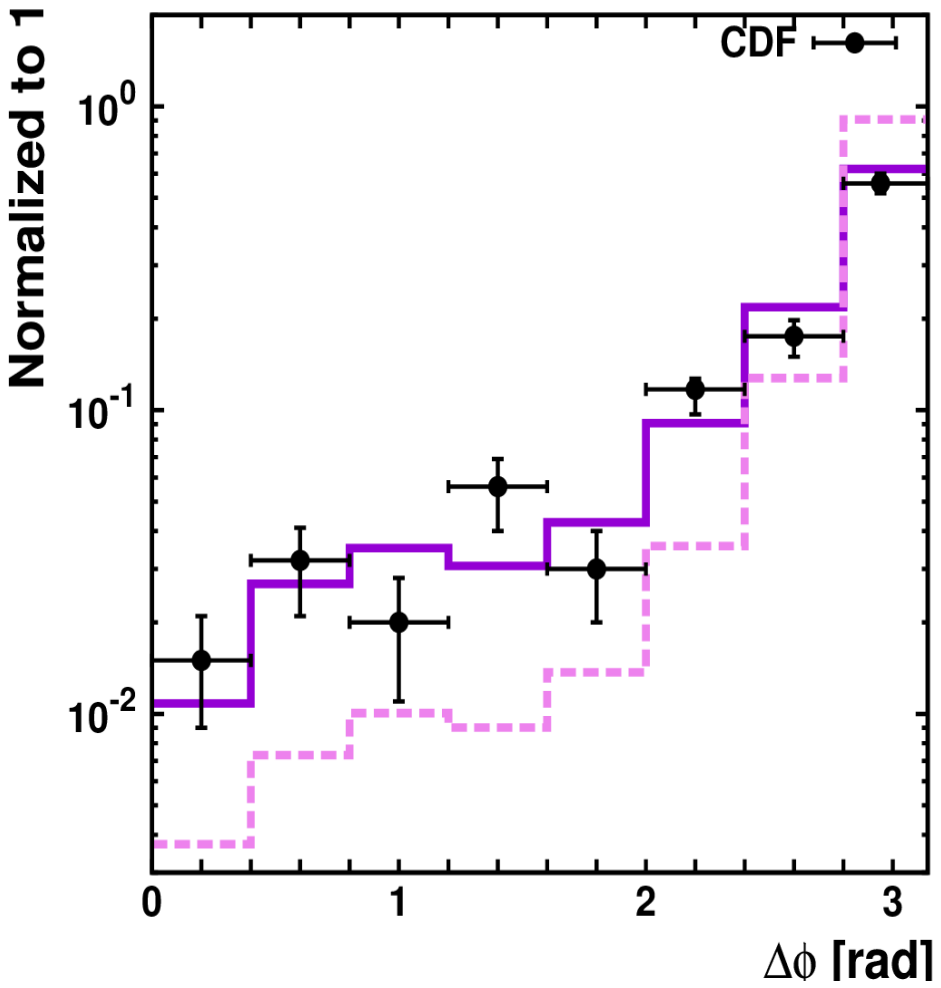

6. Differential cross section of associated prompt photon and μ-meson production $p\bar{p}\to\gamma\mu X$ as a function of the azimuthal angle difference at Tevatron energies ($\sqrt{s}$=1.8 TeV). The experimental data are of CDF ($|y^{\gamma}|<0.9$, $|y^{\mu}|<1.5$, $p_T^{\mu}>20$ GeV, $17<p_T^{\gamma}<40$ GeV). The dotted line represents the collinear QCD predictions

Numerical results

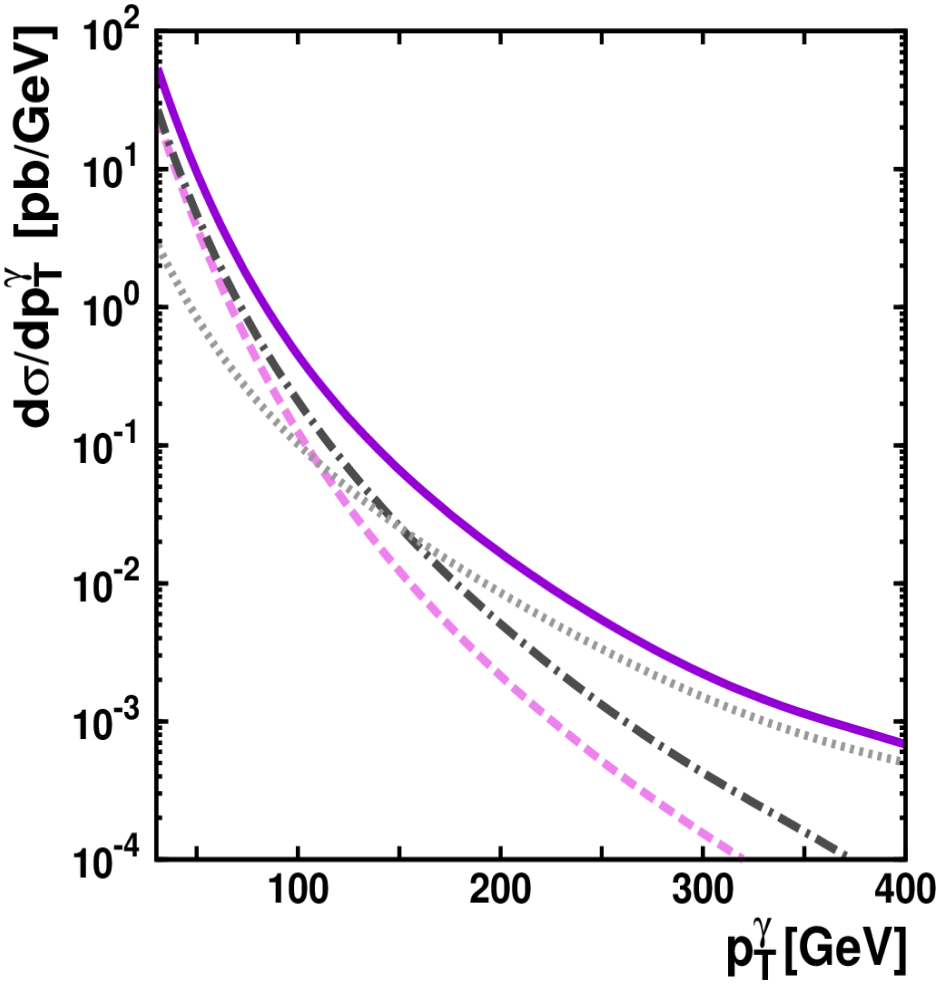

7. Differential cross section of associated prompt photon and b-jet production $pp \to \gamma b X$ at LHC energies ($\sqrt{s}$=7 TeV, $|y^\gamma|<2.5$, $|y^{b\text{-}jet}|<2.5$, $25<p_T^\gamma<400$ GeV, $18<p_T^{b\text{-}jet}<200$ GeV).The dashed, dotted and dashed-dotted lines correspond to $g^*g^* \to \gamma b\bar{b}$, $q^*\bar{q}^* \to \gamma b\bar{b}$ and $q^*b \to \gamma qb$.

Numerical results

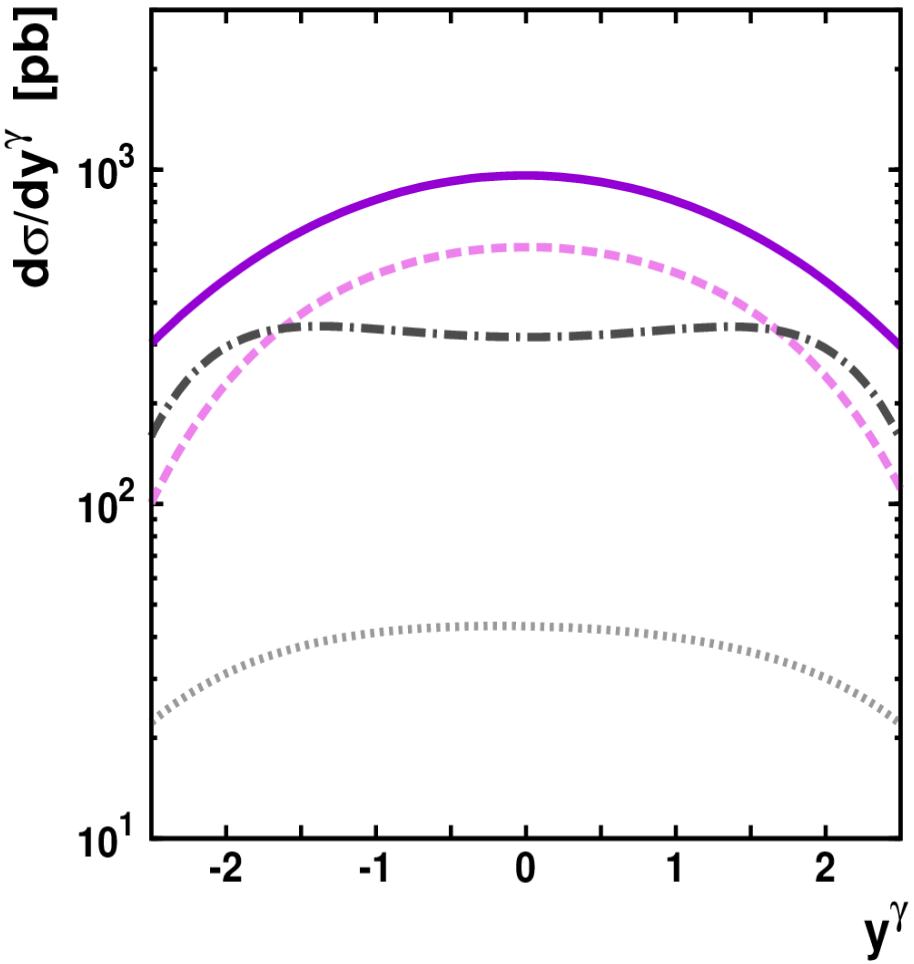

7. Differential cross section of associated prompt photon and b-jet production $pp \to \gamma bX$ as a function of y *at* LHC energies ($\sqrt{s}$=7 TeV, $|y^{\gamma}|<2.5$, $|y^{b\text{-}jet}|<2.5$, $25<p_T^{\gamma}<400$ GeV, $18<p_T^{b\text{-}jet}<200$ GeV).The dashed, dotted and dashed-dotted lines correspond to $g^*g^* \to \gamma b\bar{b}$, $q^*\bar{q}^* \to \gamma b\bar{b}$ *and* $q^*b \to \gamma qb$.

Conclusion

In the presented work process of the associated prompt photon and heavy (b, c) quark production in the k_T-factorization QCD approach at Tevatron and LHC energies has been studied.

The off-shell matrix elements for $g^*g^* \to \gamma Q\bar{Q}$, $q^*\bar{q}^* \to \gamma Q\bar{Q}$ and $q^*Q \to \gamma qQ$ subprocesses have been evaluated.

A reasonably good description of CDF and D0 data for the associated prompt photon and heavy (b, c) quark at Tevatron has been obtained. Also the associated prompt photon and μ-meson production has been studied.

The obtained results prove the applicability of the KMR unintegrated parton distribution for the description of such processes.

Back up

Off-shell quarks

In the presented work we used a method, described in the article [S.P. Baranov, A.V. Lipatov, N.P. Zotov, Phys. Rev **D 81**, 094034 (2010)]. According to this method, the off-shell quark spin density matrix has the form (in the limit of zero masses):

$$\sum_s u^s(k)\bar{u}^s(k) = x\hat{P}$$

Here *P* is the momentum of the incoming proton.

Divergencies

We do not use the concept of fragmentation functions obviously. In our approach the effect of final state radiation is already included in calculations at the level of partonic subprocess matrix elements (we have a $2 \to 3$ rather than $2 \to 2$ subprocesses). But as in the traditional approach the calculated cross sections can be split into two pieces: the direct and fragmentation contributions. They depend on fragmentation scale μ^2.

In our calculations μ is the invariant mass of the produced photon and any final quark and we restrict direct contribution to $\mu \geq M = 1\text{GeV}$ in order to eliminate the collinear divergences in the direct cross section. Then the mass of light quark m_q can be safely to zero. The numerical effects of M is really small. It is less important than other theoretical uncertainties (connected with choice of renormalization and factorization scales).